Applied Research Laboratory

Technical Report

THE HIGH REYNOLDS NUMBER FLOW THROUGH AN AXIAL-FLOW PUMP: GEOMETRY AND DATA FILES

by

W. A. Straka
W. C. Zierke

PENNSTATE

DISCLAIMER NOTICE

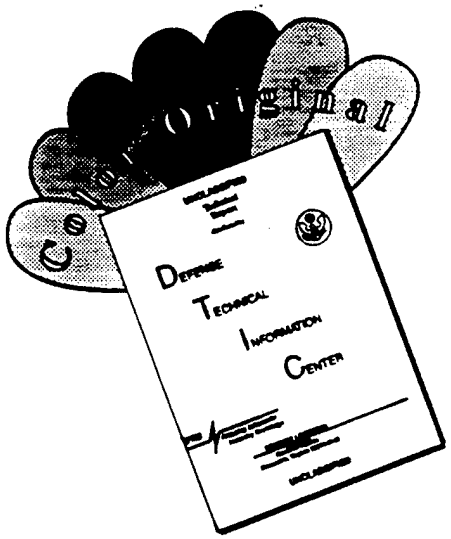

THIS DOCUMENT IS BEST QUALITY AVAILABLE. THE COPY FURNISHED TO DTIC CONTAINED A SIGNIFICANT NUMBER OF COLOR PAGES WHICH DO NOT REPRODUCE LEGIBLY ON BLACK AND WHITE MICROFICHE.

The Pennsylvania State University
APPLIED RESEARCH LABORATORY
P.O. Box 30
State College, PA 16804

THE HIGH REYNOLDS NUMBER FLOW THROUGH AN AXIAL-FLOW PUMP: GEOMETRY AND DATA FILES

by

W. A. Straka
W. C. Zierke

Technical Report No. TR 96-002
February 1996

Supported by:
Advanced Research Projects Agency

L.R. Hettche, Director
Applied Research Laboratory

Approved for public release; distribution unlimited

REPORT DOCUMENTATION PAGE

Form Approved
OMB No. 0704-0188

1. AGENCY USE ONLY (Leave blank)	2. REPORT DATE	3. REPORT TYPE AND DATES COVERED
	February 1996	

4. TITLE AND SUBTITLE

The High Reynolds Number Flow Through an Axial-Flow Pump: Geometry and Data Files

5. FUNDING NUMBERS

N00039-92-C-0100

6. AUTHOR(S)

W. A. Straka and W. C. Zierke

7. PERFORMING ORGANIZATION NAME(S) AND ADDRESS(ES)

Applied Research Laboratory
P.O. Box 30
State College, PA 16804

8. PERFORMING ORGANIZATION REPORT NUMBER

TR 96-002

9. SPONSORING/MONITORING AGENCY NAME(S) AND ADDRESS(ES)

Advanced Research Projects Agency
3701 N. Fairfax Dr.
Arlington, VA 22203-1717

10. SPONSORING/MONITORING AGENCY REPORT NUMBER

11. SUPPLEMENTARY NOTES

12a. DISTRIBUTION/AVAILABILITY STATEMENT

Unlimited

DISTRIBUTION STATEMENT A
Approved for public release
Distribution Unlimited

12b. DISTRIBUTION CODE

13. ABSTRACT (Maximum 200 words)

The high Reynolds number pump (HIREP) facility at the Applied Research Laboratory of The Pennsylvania State University (ARL Penn State) has been used to perform a low-speed, large-scale experiment of the incompressible flow of water through a two blade-row turbomachine. The objectives of this experiment were to provide a database for comparison with three-dimensional, turbulent flow computations, to evaluate engineering models, and to improve our physcial understanding of many of the phenomena involved in this complex flow field. With a complete description of the HIREP geometry, the experimental results provide an excellent test case for comparison with numerical computations. This report briefiy outlines the facility, blade row geometry, and locations where measurements were taken during the HIREP experiment. The report also introduces the reader to the available experimental and design data, as well as to the format of the contributed data bank files.

14. SUBJECT TERMS

High Reynolds Number Flow, Axial-Flow, Pump, Turbomachine
Viscous Flow, Data Bank, Data Base

15. NUMBER OF PAGES

25

16. PRICE CODE

17. SECURITY CLASSIFICATION OF REPORT	18. SECURITY CLASSIFICATION OF THIS PAGE	19. SECURITY CLASSIFICATION OF ABSTRACT	20. LIMITATION OF ABSTRACT
Unclassified	Unclassified	Unclassified	Unlimited

Abstract

The high Reynolds number pump (HIREP) facility at the Applied Research Laboratory of The Pennsylvania State University (ARL Penn State) has been used to perform a low-speed, large-scale experiment of the incompressible flow of water through a two blade-row turbomachine. The objectives of this experiment were to provide a database for comparison with three-dimensional, turbulent flow computations, to evaluate engineering modes, and to improve our physical understanding of many of the phenomena involved in this complex flow field. With a complete description of the HIREP geometry, the experimental results provide an excellent test case for comparison with numerical computations. This report briefly outlines the facility, blade-row geometry, and locations where measurements were taken during this HIREP experiment. This report also introduces the reader to the available experimental and design data, as well as to the format of the contributed data bank files.

Table of Contents

List of Tables

List of Figures

Nomenclature

A	annular area through HIREP (7.22 ft^2)
c	blade chord
C_p	static-pressure coefficient $= \dfrac{p - p_{ref}}{\frac{1}{2}\rho V_{ref}^2}$
C_{p_T}	total-pressure coefficient $= \dfrac{p_T - p_{ref}}{\frac{1}{2}\rho V_{ref}^2}$
$C_{\Delta p_T}$	total-pressure variation coefficient $= \dfrac{\Delta p_T}{\frac{1}{2}\rho V_{ref}^2}$
D	diffusion factor $= 1 - \dfrac{\bar{W}_2}{\bar{W}_1} \pm \dfrac{r_1 \bar{V}_{\theta_1} - r_2 \bar{V}_{\theta_2}}{(r_1 + r_2)\sigma \bar{W}_1}$; $+ \Rightarrow$ *stators*, $- \Rightarrow$ *rotors*
D_{tip}	rotor blade diameter
F_T	rotor shaft thrust
HIREP	high Reynolds number pump
IGV	inlet guide vane
J	advance ratio $= \dfrac{V_{ref}}{nD_{tip}}$
K_p	pressure coefficient $= \dfrac{p - p_{ref}}{\frac{1}{2}\rho U_{tip}^2}$
K_Q	torque coefficient $= \dfrac{M_Q}{\rho n^2 D_{tip}^5}$

Nomenclature (cont)

K_T	thrust coefficient $= \dfrac{F_T}{\rho n^2 D_{tip}^4}$
LDV	laser Doppler velocimeter
M_Q	rotor shaft torque
n	rotor shaft speed in revolution per second
p	static pressure
p_T	total or stagnation pressure
Q	volume flow rate
r	radius (relative to tunnel axis);
	radial coordinate
s	blade spacing
U_{tip}	rotor blade tip speed
V	velocity (relative to tunnel coordinate system)
V_{ref}	inlet reference velocity
W	relative velocity
x	axial coordinate
Y	immersion from casing endwall (Figures 9 and 12)
z	axial coordinate
Δp_T	total-pressure variation from the mean
θ	tangential coordinate
ν	kinematic viscosity

Nomenclature (cont)

ρ	fluid density
σ	blade solidity $= c \ / \ s$
ϕ	flow coefficient $= \frac{V_{ref}}{U_{tip}}$
ϕ_{vol}	volumetric flow coefficient $= \frac{Q}{nD_{tip}^3} \approx \frac{AV_{ref}}{nD_{tip}^3}$

Subscripts

∞	reference measurement
r	radial direction
ref	reference measurement
t	tangential direction
tip	rotor blade tip
z	axial direction
θ	tangential direction
∞	reference measurement

Superscripts

$\bar{}$	ensemble average
$=$	time average;
	circumferential average
$\sim$	tilda, periodic or deterministic quantity
$'$	prime, random or nondeterministic quantity

Introduction

Low-speed, large-scale experiments within multiple-blade-row machines have become increasingly important in the field of turbomachinery over the last several years. There are several reasons for this trend. The first is the increasing use of numerical prediction methods in the design, development, and analysis of multiple-blade-row machines. In order to extend the range of confidence in these numerical codes, a well-controlled experiment was needed to provide data to validate the numerical results. A second reason for this experimental trend lies in the fact that despite the great advances in numerical prediction codes, many critical calculations required by the designer cannot yet be performed by solving the governing equations from first principles. Engineering models are still required and these empirical models still need experimental data for closure. The final reason for multiple-blade-row turbomachinery experiments lies in our lack of physical understanding of many of the phenomena involved in this complex flow field. Many of these phenomena are specific to multiple-blade-row turbomachines and have not been addressed with enough detail.

None of the growing number of low-speed, large-scale, multiple-blade-row experiments has dealt with the incompressible flow of water at large blade-chord Reynolds numbers. In order to extend the range of our numerical prediction codes, flow models, and physical understanding to this incompressible flow problem, Zierke, Straka, and Taylor [1993] performed new experiments using ARL Penn State's high Reynolds number pump (HIREP). The HIREP facility can achieve blade chord Reynolds numbers as high as 6,000,000 and can accommodate a variety of instrumentation in both a stationary and a rotating frame of reference. Using HIREP, Zierke, Straka, and Taylor [1993] performed an experiment using several types of experimental techniques to document the flow field within a two-blade-row pump. Zierke, Straka, and Taylor [1993] give details of the experiment--as well as a complete analysis of all the data (including data uncertainty and limitations)-- while Zierke, Straka, and Taylor [1995], Zierke and Straka [1995], and Zierke, Farrell, and Straka [1995] summarize various aspects of the experiment.

With a complete description of the HIREP geometry, the experimental results of Zierke, Straka, and Taylor [1993] provide an excellent test case for comparison with numerical computations. This report will briefly outline the facility, blade-row geometry, and locations where measurement were taken during for this HIREP experiment. The report will also introduce the reader to the available experimental and design data, as well as the format of the data bank contributed data files. All contributed files are in a standard ASCII form. This report assumes that the reader has available the detailed report by Zierke, Straka, and Taylor [1993] so that they may reference both the figure numbers and details such as data uncertainty and experimental limitations. In order to use the provided experimental and design data to make valid and adequate comparisons, the reader must be aware of both the experimental accuracy and limitations and should not use the data blindly.

Experimental Facility

This experiment was performed in the Garfield Thomas Water Tunnel at ARL Penn State. As shown in Figure 1, this tunnel has a 4-foot diameter, 14-foot long test section which supports water velocities up to 60 ft/sec and static pressures ranging from 3 to 60 psia. Tunnel turbulence is controlled using a honeycomb placed within the settling section, 9.25 feet upstream of the nine-to-one contraction nozzle, giving a measured axial component of the freestream turbulence intensity level to be $0.11\% \pm 0.01\%$

with 95% confidence. This value was measured by Robbins [1978] using a conical hot-film probe and based on freestream velocities ranging from 20 to 60 ft/sec. Robbins [1978] also measured a longitudinal integral length scale of 0.547 $\pm$ 0.057 inches with 95% confidence--over the same velocity range. Lauchle, Billet, and Deutsch [1989] give a detailed description of the tunnel, as well as some of the basic experimental details.

Figure 2 shows a schematic of the HIREP facility. HIREP consists of a 42-inch diameter pump stage driven by a 48-inch diameter downstream turbine. The hub has a constant diameter of 21 inches which results in an annular area through the pump of $A = 7.22$ ft^2. The pump and turbine rotate together on a common shaft in the test section of the water tunnel--such that the main drive impeller of the tunnel overcomes the energy loses within HIREP. The pump stage includes a row of thirteen inlet guide vanes, a row of seven rotating blades, and three downstream support struts. The turbine stage includes a row of variable pitch control vanes, a row of rotating blades, and a downstream cruciform support strut.

The HIREP experiment included blade designs which are described in detail by Zierke, Straka, and Taylor [1993]. However for both review and emphasis, some of the important geometric characteristic should be noted again. To provide an experimental flow field in which one might expect better comparisons with numerical computations, both the inlet guide vanes and rotor blades were designed to avoid separation on the rotor blades from the standpoint of flow diffusion. The rotor blades were designed for values of diffusion factor that increased monotonically from $D = 0.12$ at the tip to $D = 0.28$ at the root. Also, the moderately-loaded rotor blades were designed to remove the swirl at the tip and with a residual swirl which increased linearly towards the hub. However, in other respects--such as cavitation performance, head rise, flow coefficient, blade numbers, and basic shapes--the design was intended to represent typical axial-flow pumps. The 13 inlet guide vanes had a chord length of 6.90 inches and a solidity ranging from 1.36 at the hub to 0.68 at the tip. The 7 rotor blades had a chord length of 11.22 inches and a solidity of 1.19 at the hub and a chord length of 10.49 inches and solidity of 0.56 at the tip. Each inlet guide vane and rotor blade trailing-edge geometry was essentially an asymmetric chisel, with the bevel of the chisel lying on the suction side of the blade and the point of the chisel being somewhat rounded off. All of the inlet guide vanes and rotor blades included fillets where the blade sections meet the endwalls. Figure 3 shows a computer-generated graphical representation of the inlet guide vanes and rotor blades as well as the coordinate system used in the experimental data. As seen in Figure 3, the rotor blades were designed with significant negative blade circumferential lean or skew--such that the suction surface points towards the hub surface. Finally, a ring mechanism was used to allow the inlet guide vanes to be circumferentially indexed in 2 degree increments over 2-1/2 blade spacings.

At their operating design point, the rotor blades rotated clockwise (looking upstream) at 260 rpm which yielded a rotor blade tip speed of $U_{tip} = 47.6$ ft/sec (using the nominal tip radius of 1.75 ft). From similarity considerations, the volumetric flow coefficient was derived as

$$\phi_{vol} = \frac{Q}{nD_{tip}^3} \approx \frac{AV_{ref}}{nD_{tip}^3},$$

where Q is the volume flow rate, n is the rotor shaft speed in revolutions per second, D_{tip} is the rotor blade diameter, and V_{ref} is the inlet reference axial velocity. This investigation was completed at the design value of $\phi_{vol} = 1.36$ with a dimensionless specific speed of $\tilde{n} = 0.89$. All data available in the data bank were obtained at this design operating condition unless otherwise stated in the data file header.

Geometry Data

To allow the reader to use the experimental results of Zierke, Straka, and Taylor [1993] as a test case for comparison with numerical computations, a complete description of the geometry is necessary. The geometry of the HIREP facility is therefore provided to the data bank in the three files shown in Table 1.

Table 1. HIREP Geometry Files

Filename	Description of File
HIREP-XR.IGS	Two-dimensional x-r view of the HIREP facility including the test section, nozzle, liner, hub, and blade locations.
HIREPIGV.IGS	IGV three-dimensional surface definition including fillets.
HIREPROT.IGS	Rotor blade three-dimensional surface definition including fillets.

Each of these files are in the Initial Graphics Exchange Specification (IGES) version 5.2 format. They were generated using Unigraphics CAD system version 9.1 with a UG/IGES version 10.4 translator. Figure 4 illustrates the two-dimensional x-r data contained in the HIREP-XR.IGS geometry file. Figure 5 illustrates two views of the three-dimensional surface data from the inlet guide vane geometry file, HIREPIGV.IGS. Similarly, Figure 6 shows two views of the three-dimensional surface data from the rotor blade geometry file, HIREPROT.IGS.

Experimental Techniques and Measurement Locations

The large-scale HIREP facility used by Zierke, Straka, and Taylor [1993] accommodates a variety of instrumentation on both a stationary and rotating frame of reference. A high-capacity, low-noise slip ring was used for many measurements in the rotating frame and an incremental, optical shaft encoder provided both rotor angular positions and speed. The water temperature was measured in the settling section with a resistance-temperature device. For the entire experiment, the temperature ranged from 75°F to 92°F, with an average value of about 85°F. This average temperature yields the following average properties given in Table 2.

Table 2. Experimental Average Fluid Properties

Property	Value
density, ρ	1.932 *slugs/ft*^{3}
kinematic viscosity, ν	0.000008755 *ft*^{2}*/sec*
vapor pressure, p_v	0.5968 *psia*

As stated previously all the experimental measurements available in the data bank were acquired at specific values of ϕ_{vol}. The tunnel was also pressurized during all testing to eliminate cavitation. To measure tunnel conditions a wall-static pressure tap--Kiel probe combination was used. The static pressure tap was located 58.6% chord axially upstream of the IGV leading edge in the region of the duct where both the hub and outer liner are cylindrical. This tap was used to record the reference static pressure, P_{ref}. Far upstream in the settling section of the tunnel, we measured a reference total pressure, $P_{T_{ref}}$, with a Kiel probe. These two pressures along with the measured water density where used to determine a reference velocity. All the data present in the available data files are at the design values unless otherwise noted in the file header. The nominal test conditions are as are shown in Table 3. Again, it should be noted that all the data availabie in the data bank were taken at these nominal values unless otherwise noted in the file header.

Table 3. Nominal Reference and Operating Conditions for Experimental Results

Property	Nominal Value
Reference Velocity, V_{ref}	35.0 *ft/sec*
Volumetric Flow Coefficient, ϕ_{vol}	1.36
Rotor Rotational Speed	260 *rpm*
Reference Static Pressure, p_{ref}	43.2 *psia*

Rotor Shaft Torque and Thrust Measurements

Force measurements are important for determining the mechanical power required to operate the pump at various flow conditions. In order to measure the rotor shaft torque measurements, two 700-ohm strain gauges were mounted to each arm of a four-active-arm Wheatstone bridge on the inside of the rotor shaft. The gauge measured the shear strains in the shaft wall. Similarly, to measure the rotor shaft thrust, two 240-ohm strain gauges were mounted to each arm of a four-active-arm Wheatstone bridge which was bonded to the rotating hub flange. Data were taken for a series of flow coefficients.

The design values of the rotor torque coefficient, K_Q, and thrust coefficient, K_T, at $\phi = 1.36$ are 0.301 and 0.772, respectively. Zierke, Straka, and Taylor [1993] give many details with regards to the calibration procedure and data accuracy. However, it should be noted here that although the torque measurements provided very accurate data, problems in the thrust measurement provided less than desirable results.

Blade Static-Pressure Measurements

In order to measure the time-averaged static-pressure distributions, pressure taps were machined into both the inlet guide vanes and rotor blades. One inlet guide vane included a total of 40 pressure taps on its suction surface only. The adjacent vane across the same blade passage also included 40 pressure taps, however these taps were on its pressure surface. The pressure taps were placed on each of the blade surfaces with a pattern of 5 spanwise rows corresponding to nominal locations of 10%, 30%, 50%, 70%, and 90% span. The taps were individually offset slightly from these nominal spanwise positions, as illustrated in Figure 7. This was done to help protect the blades from being locally overstressed in a single plane and to prevent any possible contamination of the pressure measurements from on tap due to flow disturbances from the upstream tap. In a similar fashion, a single rotor blade passage was also instrumented to include 40 pressure taps per surface. Locations of these pressure taps are shown in Figure 8. As explained in detail by Zierke, Straka, and Taylor [1993], the overall uncertainty in measuring the blade static pressures ranged from 0.06 psi over regions of minimal streamwise pressure gradients to 0.13 psi over regions of large pressure gradients, as might be found at 90% span on the rotor blade suction surface. This overall uncertainty in pressure measurement would result in a uncertainty in pressure coefficient on the order of $K_p = \pm 0.009$.

Slow-Response Pressure Probes

Various slow-response pressure techniques--including static-pressure taps, five-hole probes, and Kiel probes--were used to acquire both three component velocity data and pressure data at various locations within HIREP. As was mentioned previously, the tunnel and HIREP operating conditions were obtained using a Kiel probe/static-pressure tap combination.

Five-hole probes were also used to measure the static and stagnation pressures radially across the flow duct from the outside tunnel liner to the hub. These five-hole probes were also calibrated and capable of resolving the three components of velocity. The five-hole probes was used in conjunction with a strongback support which spanned the duct from tunnel liner to hub. This allowed the probe itself to be transversed across the test section with minimal bending, vibration, or fatigue effects. Radial surveys were completed with a five-hole probe at locations of 37.0% chord upstream of the IGV leading edge and a 49.7% chord downstream of the IGV trailing edge. At each of these locations, measurements were made at approximately 50 radial positions. Figure 9 illustrates the locations where measurements were completed. Zierke, Straka, and Taylor [1993] completed a detailed analysis of measurement uncertainties. To summarize, the uncertainty in total velocity, $\bar{V}$, with 95% confidence for the upstream and downstream measurements was 3.1% and 7.7%, respectively.

While the radial five-hole probe survey provided excellent resolution in the radial direction, they gave poor resolution in the circumferential direction, even using the IGV ring mechanism. In order to improve this circumferential resolution, a rotating rake of five-hole probes was used. The rake

consisted of a 21-inch diameter hub that carried six five-hole probes, each which included splitter vanes which reduced vortex shedding and probe vibration. Figure 10 shows how a typical rake probe was positioned between the blade rows in the HIREP facility. Axially, the rake measurements were acquired at the same location as the five-hole probe surveys, as shown in Figure 9. Data was obtained for 11 radial positions as is also shown in Figure 9. The circumferential resolution of these measurements was 0.373 degrees. Considering the probe size (0.066 inches), the spatial resolution of the probe measurement varies from 0.344 degrees at 4.8% span to 0.185 degrees at 95.2% span. In order to adequately compare to the experimental values, the reader is cautioned to consider the circumferential and spatial resolutions of the measurements and its possible averaging effects, especially on the wake depths. Again Zierke, Straka, and Taylor [1993] completed a detailed uncertainty analysis for the rake five-hole probe measurements. To summarize, the following uncertainties with 95% confidence were calculated as follows: $V_z = \pm 0.9$ ft/sec; V_r, $V_\theta = \pm 0.3$ ft/sec; p, $p_T = \pm 0.06$ psi.

Finally, time-averaged total pressure measurements were acquired 32.2% rotor tip chord axially downstream the rotor tip trailing edge using a radial Kiel probe. As with the radial surveys using five-holes probes, the Kiel probes moved within a strongback support. Data were acquired at approximately 40 radial locations across the duct. Data were obtained for two circumferential positions of the inlet guide vanes and, during these measurement, a static-pressure was taken on the outer liner wall at the same 32.2% rotor tip chord location. Again, the positions of the measurements are shown in Figure 9. The uncertainty of this pressure measurement was $C_p = \pm 0.005$ with 95% confidence.

Fast-Response Pressure Probe

A fast-response total-pressure probe was designed and used to measure the wakes and vortices associated with the rotor blades. Figure 11 illustrates the design of this fast-response total pressure probe. Zierke, Straka, and Taylor [1993] give further details of the probe design, calibration, and operation procedures. It should be pointed out that this probe was capable of continuously measuring data with a response time fast enough to resolve the total pressures for instantaneous angular positions of the rotor--positions measured with the optical encoder. However, as with most piezoelectric transducers of the type used, the probe was unable to measure the mean value of pressure. It did however provide excellent measurements of the total-pressure variation about the mean. As with the slow-response Kiel probe, the fast-response total-pressure probe moved within a strongback support. Measurements were taken at the same axial plane as the slow-response Kiel probe--32.2% chord downstream of the rotor tip trailing-edge for approximately 40 radial locations spanning the duct.

Laser Doppler Velocimeter

A laser Doppler velocimeter (LDV) was used to acquire nonintrusive measurements of the flow field upstream and downstream of the rotor blade row. A two-component LDV system was employed allowing measurements of both the tunnel axial, V_z, and tangential, V_θ, velocity. All measurements were made on the test section centerline through a specially design optical window with the IGV index set at a constant position to eliminate the presence of IGV wakes in the measurement volume. The specially designed window had an inner contour which matched that of the liner (i.e. radius of 21 inches) and an outer radius of 63.54 inches. The two radii of curvature were required to produce a near-zero magnification cylindrical lens for the laser optical system. In other words, the window

allowed both the beams for each of the two components to cross at the same location. In actuality, measurements of the component cross-over locations showed that the tangential component measurement volume tended to be slightly closer to the outer liner.

The data were collected using a field point measurement method. In this procedure, the measurement volume remains stationary and each LDV measurement sample is tagged with the angular position of the rotor--via the optical shaft encoder and a rotating machinery resolver. Typically, for every position of the LDV measurement volume, a total of 100,000 samples were obtained, of which approximately 50% were axial velocity and the other 50% tangential. Figure 12 shows the approximate locations at which LDV data were acquired. Radial surveys were completed at locations of 28.6% rotor tip chord upstream of the rotor tip leading edge as well as at 4.8%, 21.4%, and 32.2% rotor tip chord downstream of the rotor tip trailing edge. Also, data were obtained at approximately 76.2% span with an axial survey upstream of the rotor leading edge and downstream of the rotor trailing edge.

The files available in the data bank include both the circumferentially-averaged and "binned" (i.e., encoded into discrete storage windows of rotor position) velocity data. The reader is cautioned when using either type of data for comparisons to numerical result. It should remembered that all the LDV data was obtained at a single index position of the inlet guide vanes which was chosen to eliminate the presence of IGV wakes in the measurement volume. As a result, the averaged data will not account for the effects of variations across the IGV passages and may tend to give slightly higher values than an actual circumferential average. Similarly, the circumferentially binned data do not contain the effects of IGV wakes, although they are tagged with a circumferential position or bin. The reader must remember that this bin position is in reality just a tag of the relative position of the rotor and does not indicate the location relative to any stationary structure, including the inlet guide vanes. Finally, when using the circumferentially binned data, the reader must also remember that each bin has some finite dimension (either 0.5° or 1.0°) and, as with the five-hole probe rake data, possible spatial averaging does occur, especially in the wake depths.

The data included in the data bank include the location of the measurement, the mean velocity, and many other statistical values such as deterministic unsteadiness. For an explanation of this statistical analysis, the reader is again asked to refer to the descriptions by Zierke, Straka, and Taylor [1993]. That report also contains some information on both the precision and bias errors of the LDV measurements. The precision errors in the mean velocity measurements range from 0.1% to 2.4%, with the larger errors corresponding to regions with high turbulence levels. Similarly, the precision errors in the turbulence intensities range from 6.0% to 8.5%.

Contributed Data Files

The majority of the experimental and design data presented by Zierke, Straka, and Taylor [1993] has been made available as a test case for comparison with numerical computations or for further analysis. To use this data, the reader should have available the detailed report by Zierke, Straka, and Taylor [1993] or the summary article by Zierke, Straka, and Taylor [1995] so that they may reference the figure numbers, analysis, and details such as data uncertainty and experimental limitations. In order to use the provided experimental and design data to make valid and accurate comparisons, the reader must be aware of both the experimental accuracy and limitations and should not use the data blindly.

Table 4. Data File Header Layout

```
TITLE:
AUTHORS:
JOURNAL PAPER FIGURE(S):
PSU/ARL TR 93-12 FIGURE(S):
**********************************************************************
DATA TITLE:
MEASUREMENT TYPE:
MEASUREMENT LOCATION:

NOMINAL CONDITIONS:
        .
        .
        .
DATA COLUMNS:
 1 --
 2 --
        .
        .
        .
**********************************************************************
```

Data File Format

Each of the files contained in the data bank, with the exception of the geometry files previously mentioned, have been generated on a MS-DOS compatible PC in ASCII format. Each file contains a header with the format/section information as shown in Table 4.

An example file header and data file is also shown in Figure 13. The first two entries, **TITLE:** and **AUTHORS:**, in the file header are self explanatory and are just the title of the investigation and the authors. These are the same in each of the data files. The next entry, **JOURNAL PAPER FIGURE(S):** shows the figures number(s) from Zierke, Straka, and Taylor [1995] which contain the data given in the file. Similarly, the fourth entry, **PSU/ARL TR 93-12 FIGURE(S):**, contains the figure number(s) from Zierke, Straka and Taylor [1993] in which the data was used.

The next section of the header is separated by a line of asterisks. The fifth entry, **DATA TITLE**, gives the title of the data file and **MEASUREMENT TYPE** briefly explains the method by which the data was obtained or calculated. In **MEASUREMENT LOCATION** the location or position where the data acquired at is given. This is typically given in a percent chord from some known geometric feature such at a blade leading edge. The next entry, **NOMINAL CONDITION**, contain multiple lines of test conditions used when obtaining the data or parameters necessary for understanding the data such as geometric dimensions. For the example shown in Figure 13, information such as the reference velocity, water density, rotor diameter, and annulus flow area are given. The final entry in the file header, **DATA COLUMNS**, describes the data for each of the columns in the data files. This section

also explains the definition of any property given in one of the data column. Finally, the header is ended with a line of asterisks and is followed by columns of numerical data which match the number columns which appears in the **DATA COLUMNS** header entry.

Data Files

The experimental and design data contained in this data bank is supplied in a total of 157 files totaling over 4.8 megabytes. The geometry files mentioned earlier total over 2.1 megabytes and are given in 3 IGES files. To allow easier access to specific parts of the database, a data file/figure cross-reference is supplied in the file **FILELIST.TXT**. The file contains the filenames for all the files that are included in the HIREP data bank. These files are referenced with the figure numbers from both references. (Zierke, Straka and Taylor [1993,1995]) A copy of **FILELIST.TXT** is shown in Figure 15.

Access to Data

The geometry definition and experimental and design data can be accessed through the ASME *Journal of Fluids Engineering* (JFE) electronic Journal Data Bank. More information on the JFE Data Bank and directions on how to link with the Data Bank and transfer a file are included in the last page of each issue. The current method to link to the electronic JFE server is the Internet by using either telnet or the World Wide Web (WWW) at the following locations:

1) telnet scholar.lib.vt.edu
2) http://scholar.lib.vt.edu

where, when prompted one must enter the following login and password:

login: "jfe"
password: "online"

Conclusions

The HIREP experimental measurements provide an excellent database for comparisons with three-dimensional, turbulent, incompressible flow computations as long as the experimental limitation are taken into account. The database will also provide excellent empirical data for both engineering model formulation and validation. Most of the experimental results and design calculations from the axial-flow pump experiment conducted and analyzed by Zierke, Straka, and Taylor [1993] have been added to this *Journal of Fluids Engineering* data bank. The data bank contributions also include the geometry definition contained in three IGES standard files. The data contributed includes various measurements acquired upstream, between, and downstream of a two blade row axial-flow pump stage. These data were obtained using force cells, blade static-pressure taps, slow-response pressure probes, fast-response pressure probes, and laser Doppler velocimetry.

References

Lauchle, G. C., Billet, M. L., and Deutsch, S., "High-Reynolds Number Liquid Flow Measurements," *Frontiers in Experimental Fluid Mechanics*, pp. 95-157, edited by M. Gad-el-Hak, Springer-Verlag Berlin Heidelberg, 1989.

Robbins, B. E., "Water Tunnel Turbulence Measurements behind a Honeycomb," *Journal of Hydronautics*, Vol. 12, pp. 112-128, 1978.

Zierke, W. C., Farrell, K. J., and Straka, W. A., "Measurements of the Tip Clearance Flow for a High Reynolds Number Axial-Flow Rotor," Transactions of the ASME: *Journal of Turbomachinery*, Vol. 117, October 1995.

Zierke, W. C., and Straka, W. A., "Surface Flow Visualization and the Three-Dimensional Flow in an Axial-Flow Pump," to appear in AIAA *Journal of Propulsion and Power*.

Zierke, W. C., Straka, W. A., and Taylor, P. D., "The High Reynolds Number Flow Through an Axial-Flow Pump," Penn State/Applied Research Laboratory Technical Report, TR 93-12, November 1993.

Zierke, W. C., Straka, W. A., and Taylor, P. D., "An Experimental Investigation of the Flow through an Axial-Flow Pump," Transactions of the ASME: *Journal of Fluids Engineering*, Vol. 117, pp. 485-490, September 1995.

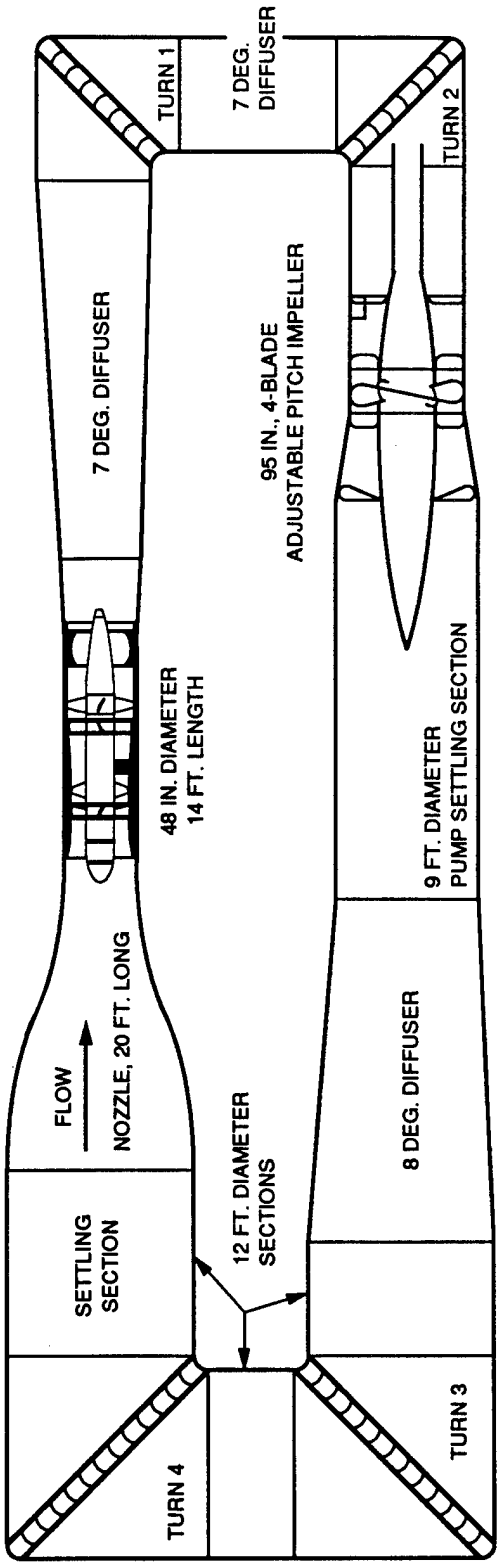

Figure 1. Garfield Thomas Water Tunnel

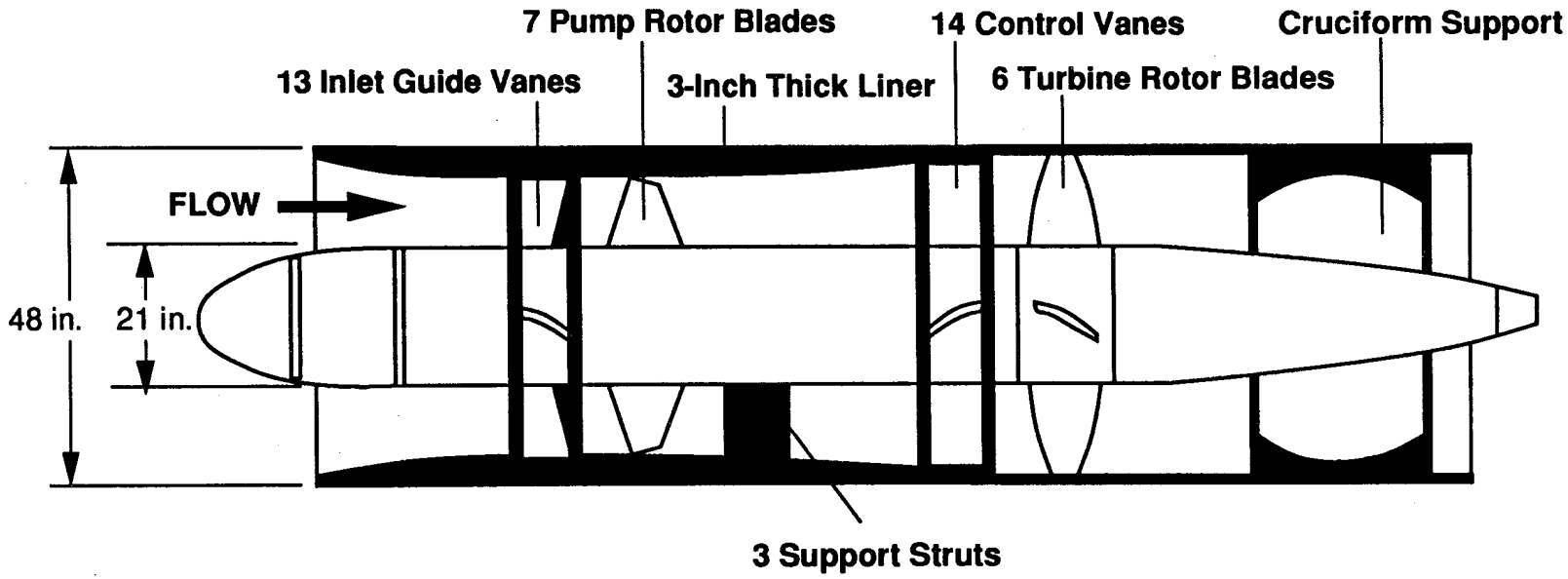

Figure 2. High Reynolds Number Pump Facility

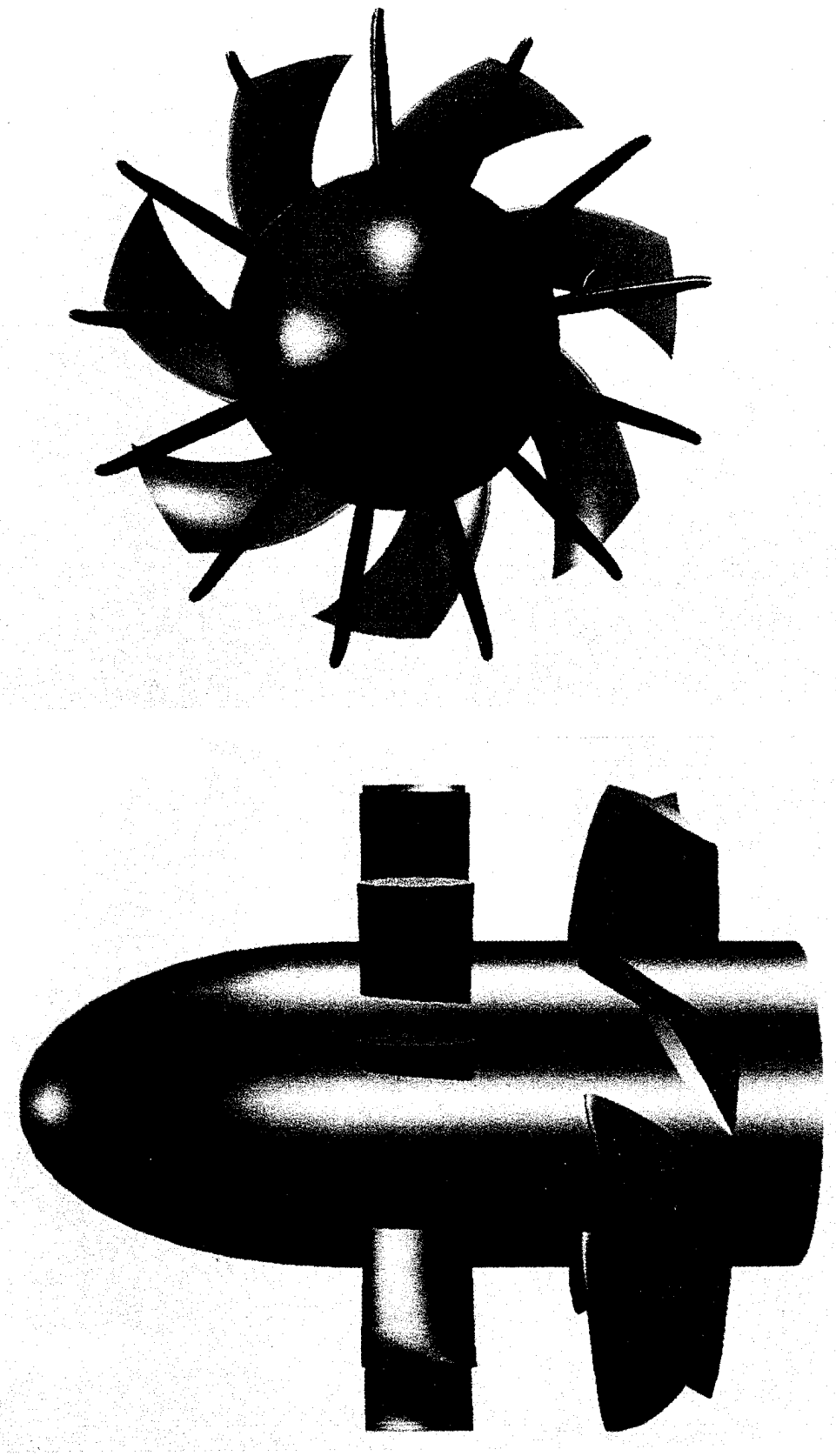

Figure 3. Computer Generated Graphical Image of the HIREP Inlet Guide Vanes and Rotor Blades
(a) Downstream and Inboard Views

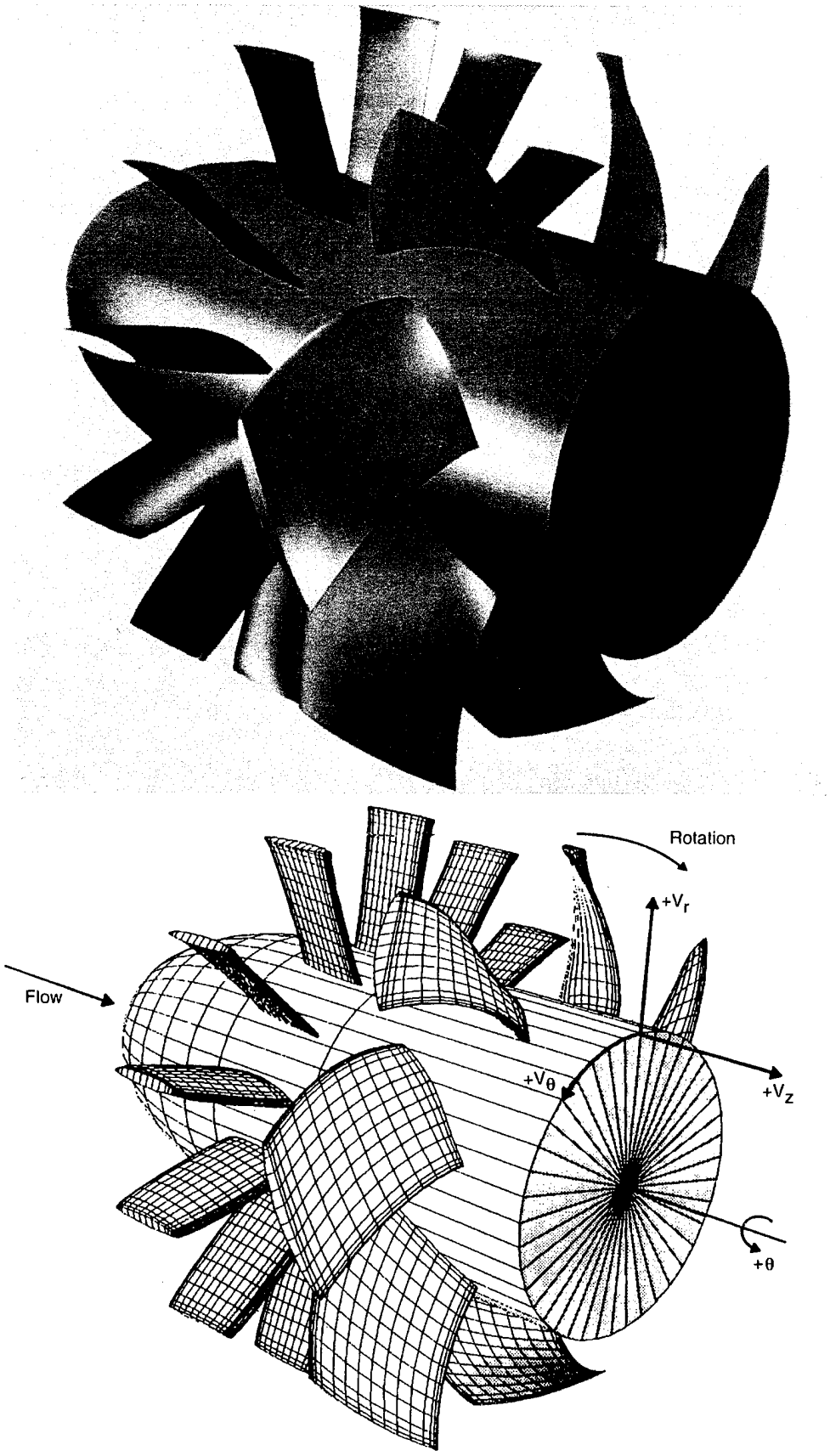

Figure 3. Computer Generated Graphical Image of the HIREP Inlet Guide Vanes and Rotor Blades (b) Isometric View with Coordinate System

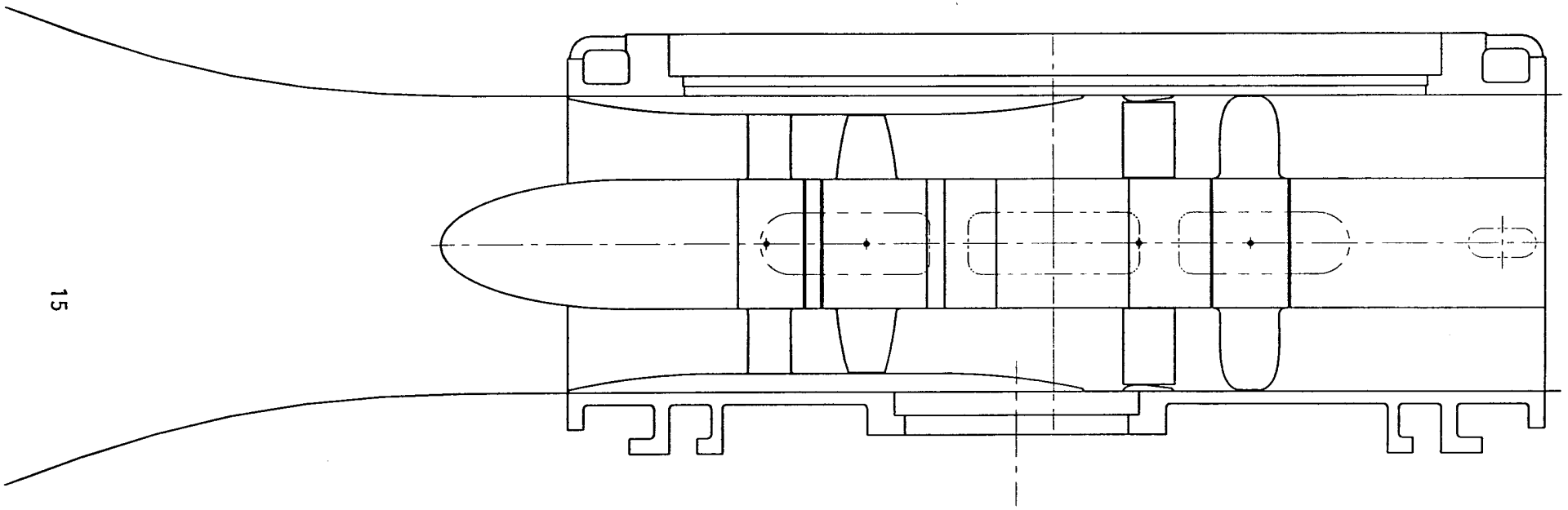

Figure 4. Two-Dimensional x-r View of Data Contained in Geometry File: HIREP-XR.IGS

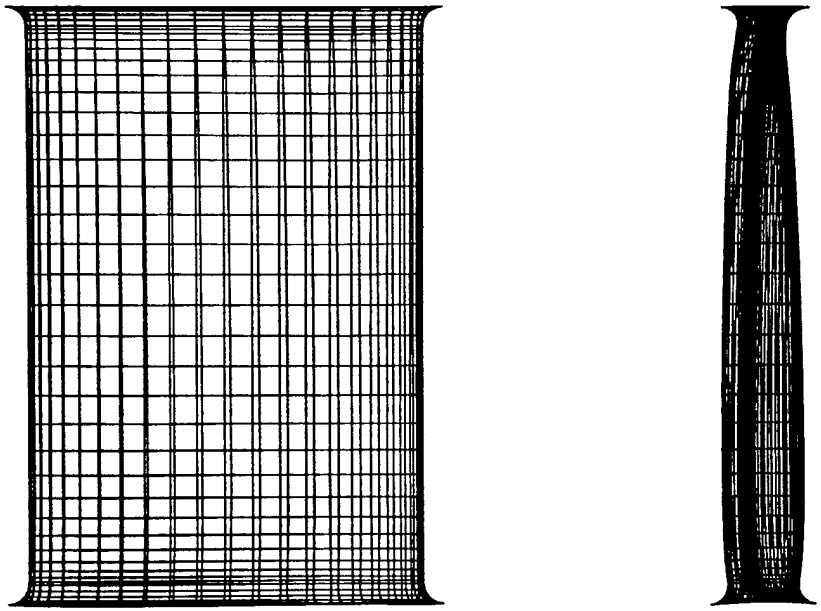

Figure 5. Illustration of Three-Dimensional Inlet Guide Vane Surface Data Contained in Geometry File: HIREPIGV.IGS

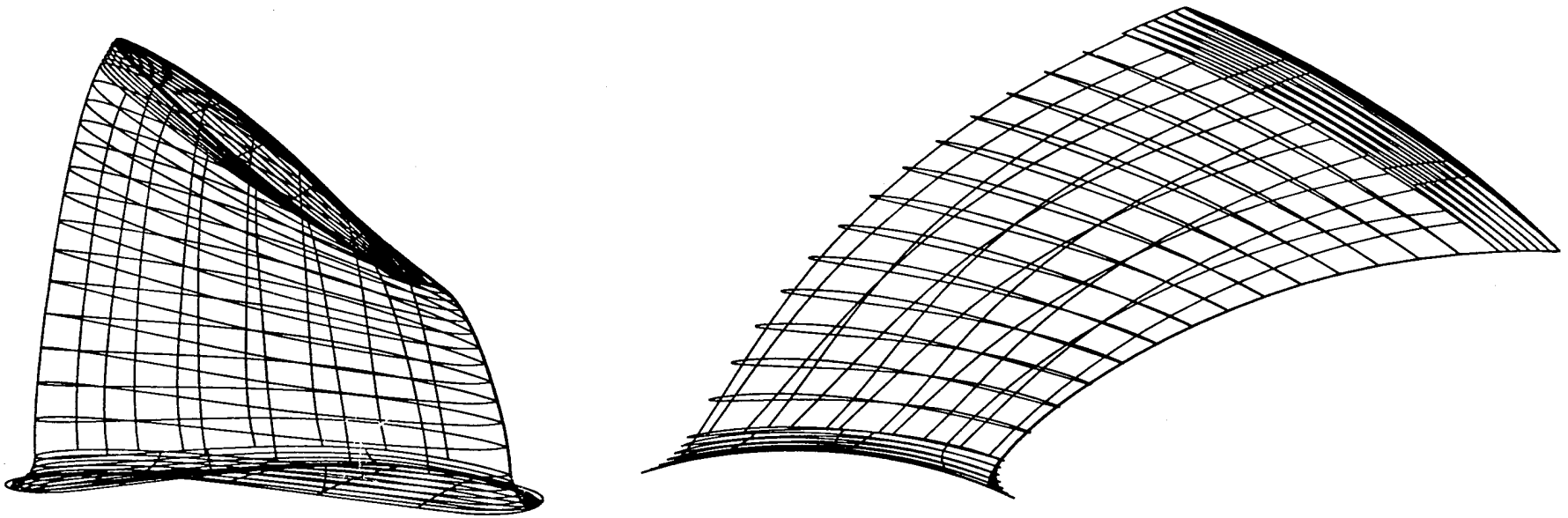

Figure 6. Illustration of Three-Dimensional Rotor Blade Surface Data Contained in Geometry File: HIREPROT.IGS

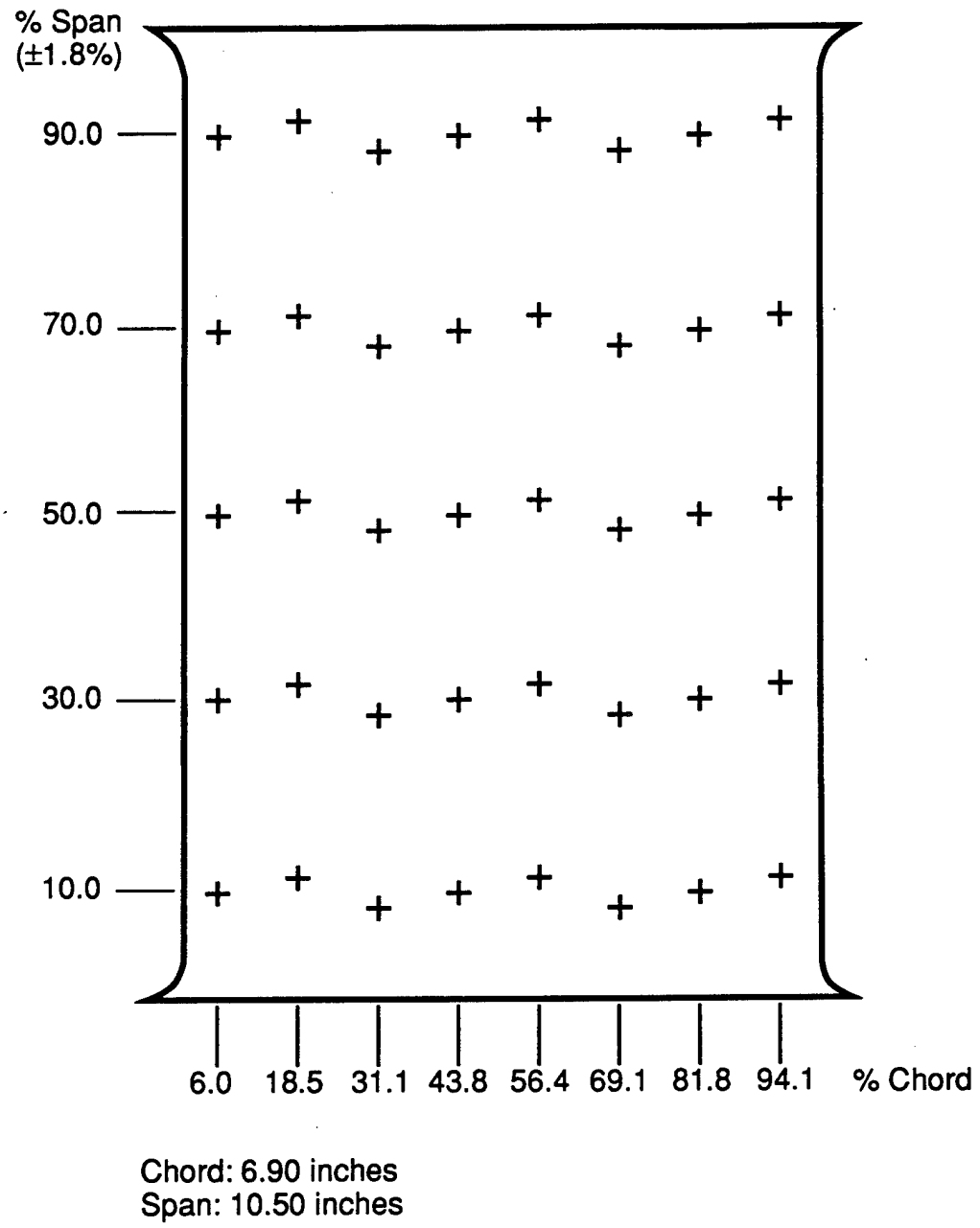

Figure 7. IGV Static-Pressure Tap Locations

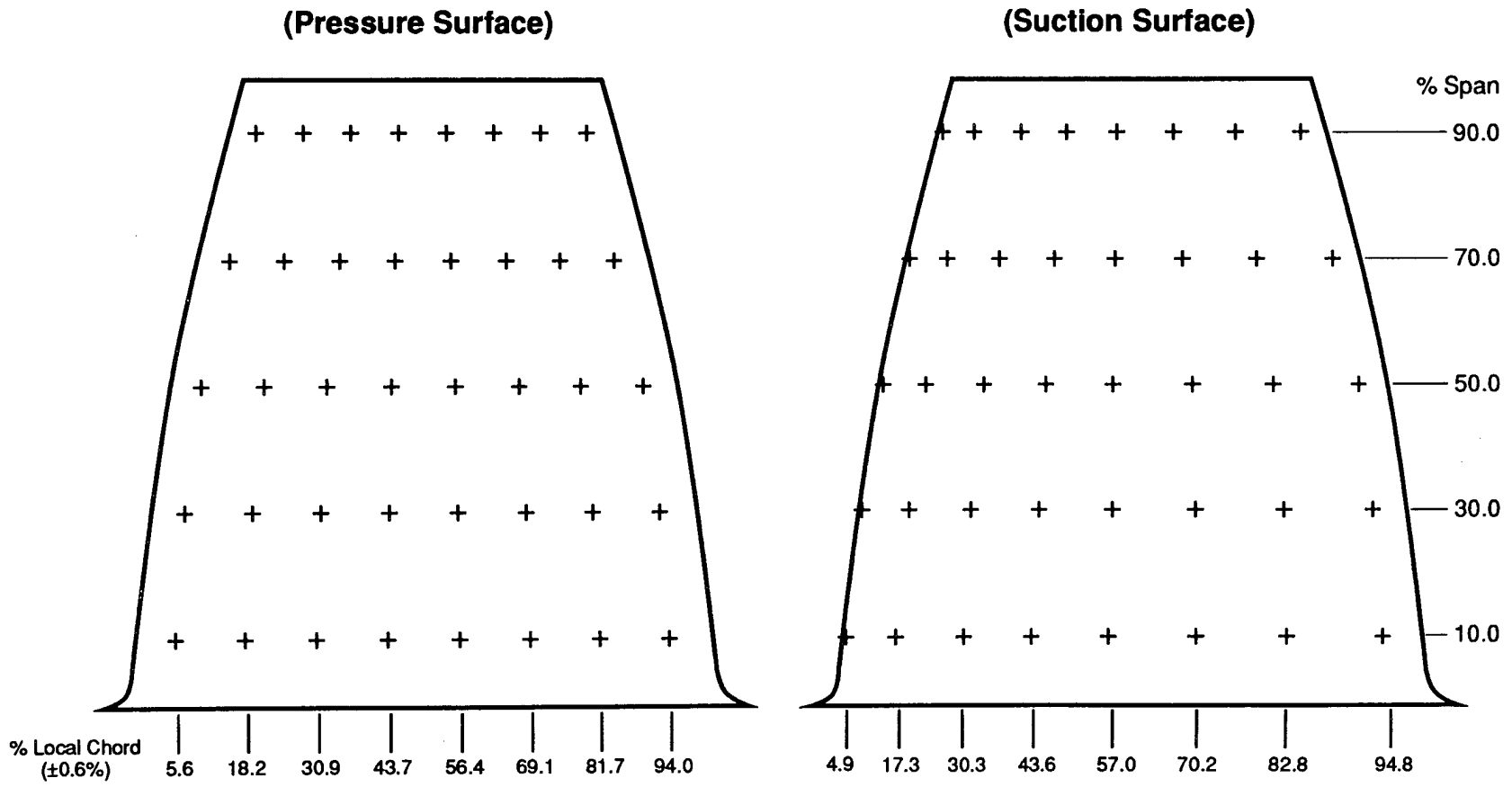

Figure 8. Rotor Blade Static-Pressure Tap Locations

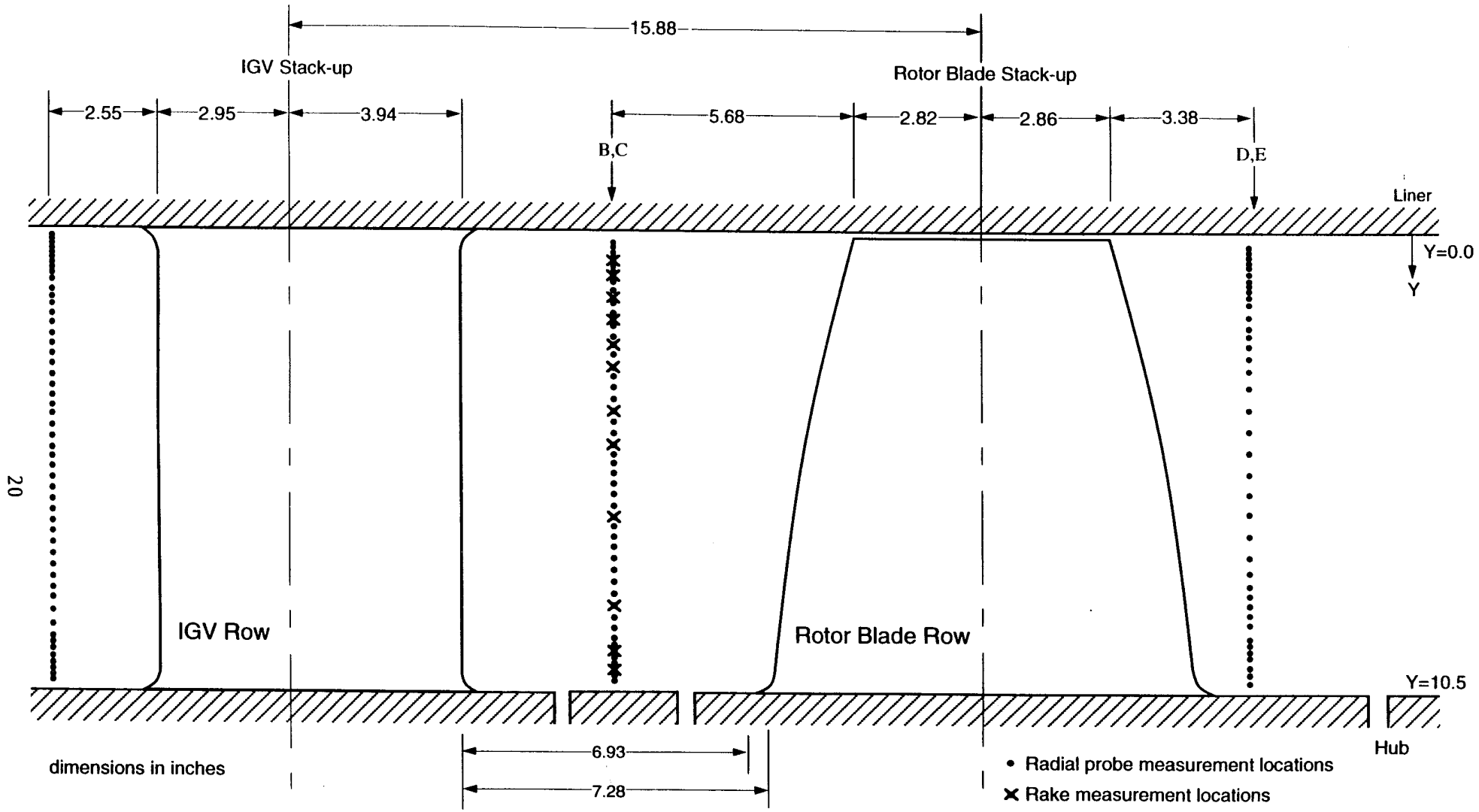

Figure 9. Pressure Probe Measurement Locations

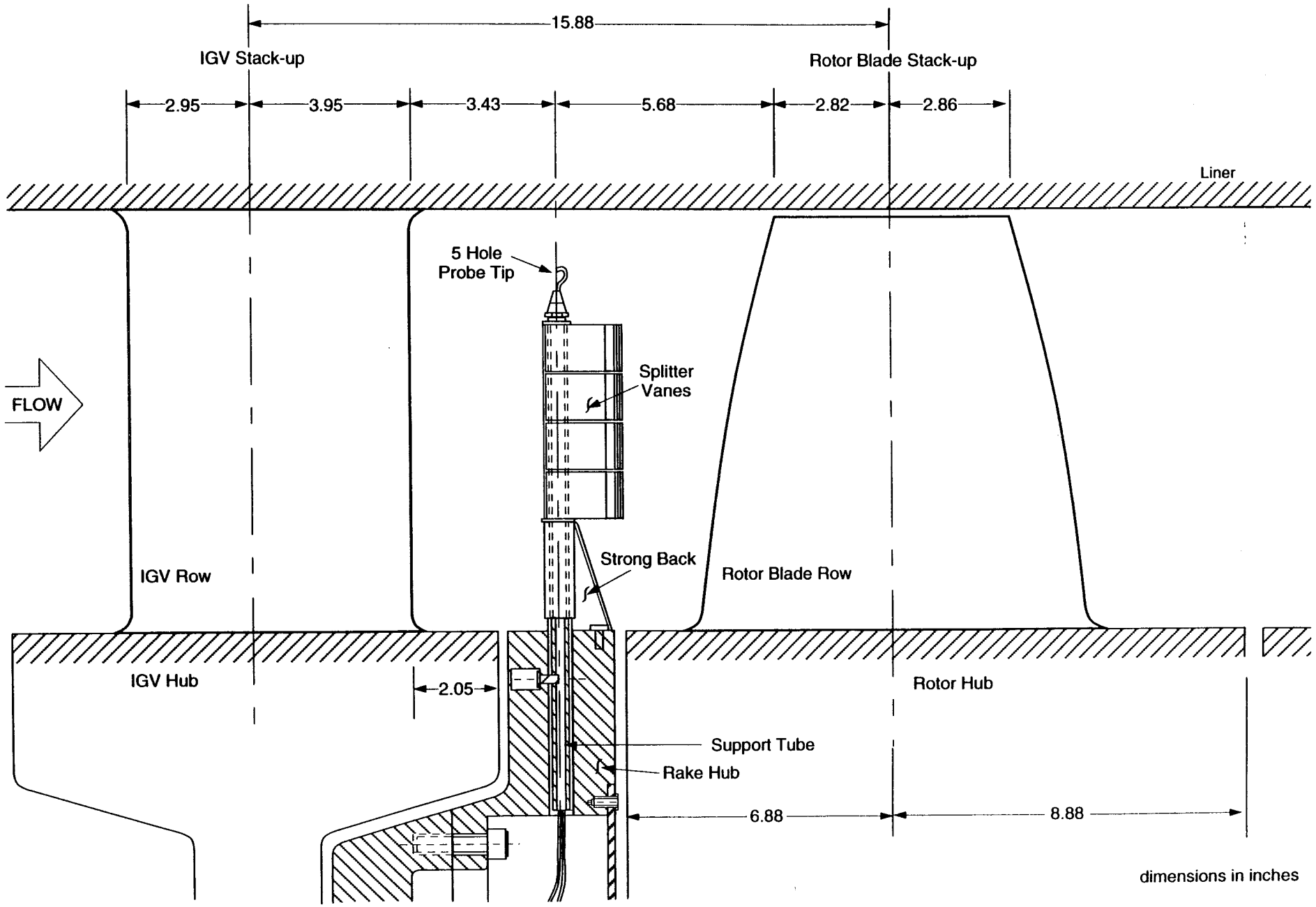

Figure 10. Sample Probe Within the Five-Hole Probe Rake

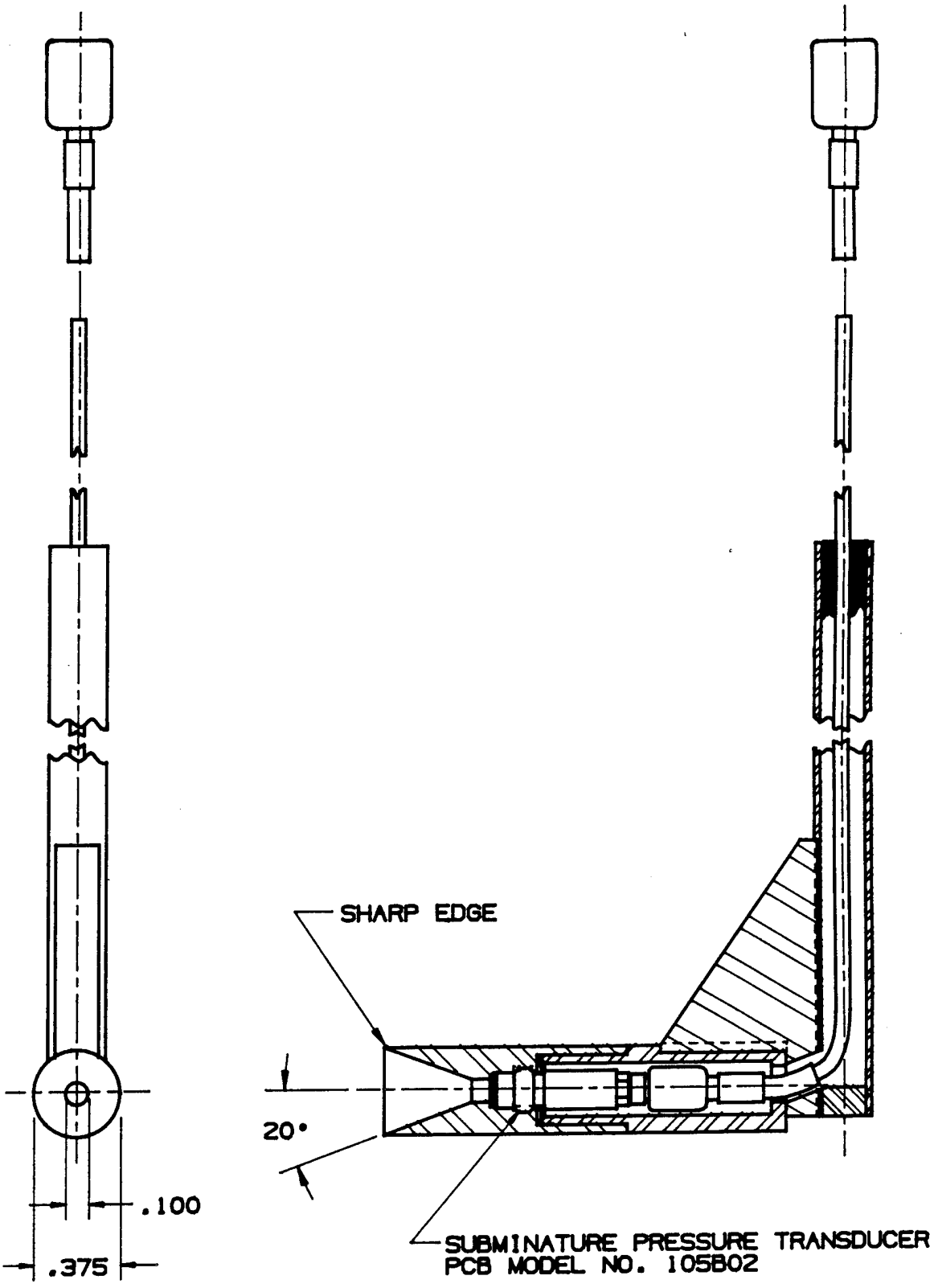

Figure 11. Schematic of Fast-Reponse Total-Pressure Probe

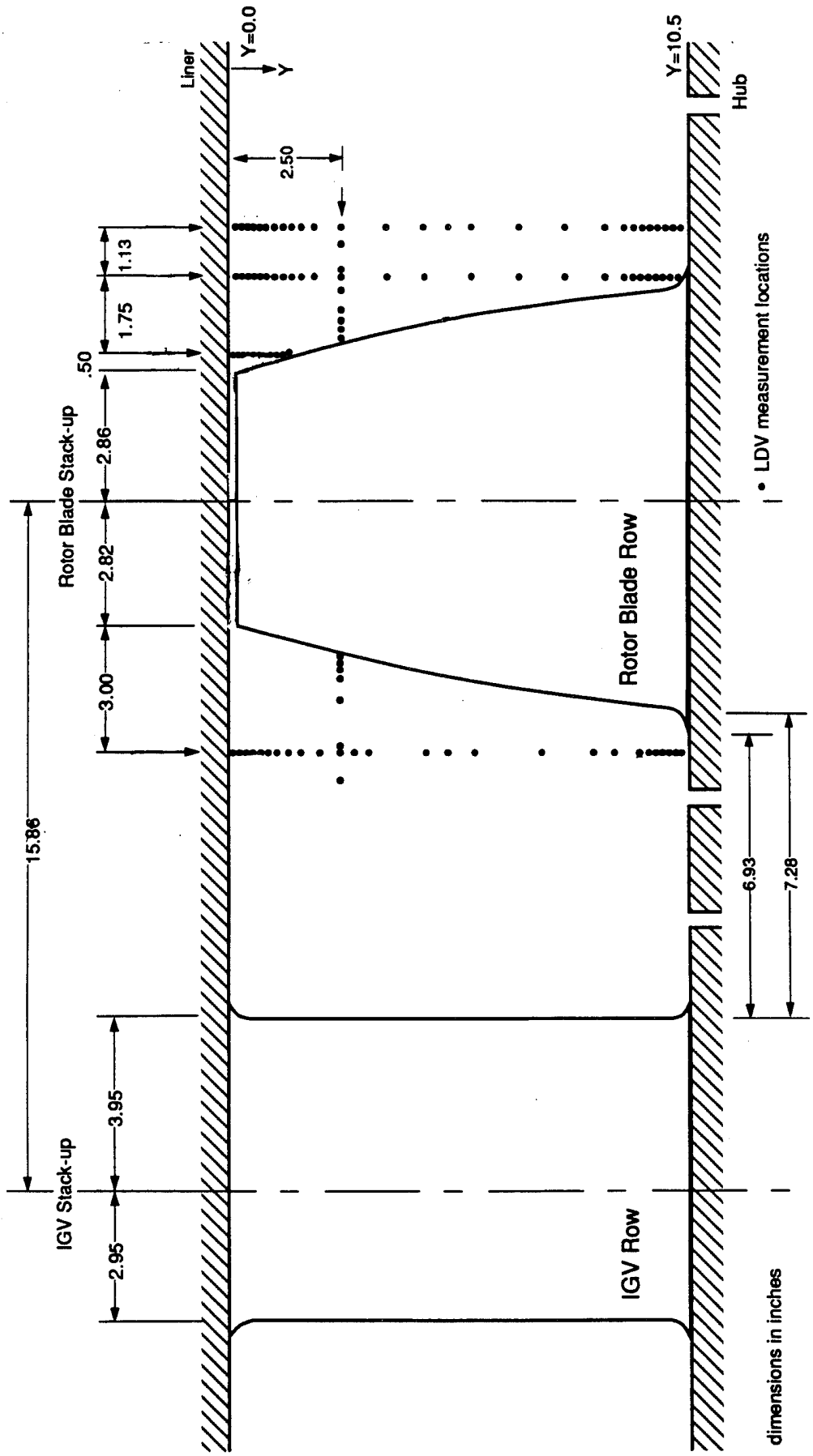

Figure 12. LDV Measurement Locations

```
TITLE:  An Experimental Investigation of the Flow through an Axial-Flow Pump
AUTHORS:  Zierke, Straka, and Taylor
JOURNAL PAPER FIGURE(S):  7
PSU/ARL TR 93-12 FIGURE(S):  46, 47
********************************************************************************
DATA TITLE:  Variation of Rotor Shaft Thrust and Torque with Flow Coefficient
MEASUREMENT TYPE:  strain guage force cells
MEASUREMENT LOCATION:  rotor blade row hub flange
NOMINAL CONDITIONS:
  vref = 35.0 ft/sec
  pref = 43.2 psia
  rho  = 1.932 slugs/ft^3
  rotor rpm  = between 235 and 292 depending on flow coefficient
  n = rotor shaft speed in revolutions per second
  rotor tip speed, Utip = variable depending on rotor rpm
  rotor diameter, D  = 1.75 ft
  annulus flow area, A = 7.22 ft^2
DATA COLUMNS:
  1 -- Volumetric Flow Coefficient, = (A * vref) / (n * D^3)
  2 -- Flow Coefficient, = (vref) / (Utip)
  3 -- Thrust Coefficient, = Thrust / (rho * n^2 * D^4)
  4 -- Torque Coefficient, = Torque / (rho * n^2 * D^5)
********************************************************************************
1.21100     0.65442     1.04400     0.31760
1.21100     0.65442     1.03600     0.31700
1.21100     0.65442     1.02500     0.31780
1.21200     0.65496     1.02400     0.31700
1.21300     0.65551     1.03100     0.31610
1.21300     0.65551     1.03300     0.31690
1.21300     0.65551     1.02700     0.31740
1.21400     0.65605     1.05700     0.32090
1.21400     0.65605     1.03900     0.31770
1.21400     0.65605     1.04500     0.31740
1.21400     0.65605     1.05900     0.31950
1.21500     0.65659     1.04300     0.32070
1.21500     0.65659     1.06100     0.31980
1.21500     0.65659     1.03200     0.31730
1.21500     0.65659     1.03400     0.31640
1.21600     0.65713     1.04100     0.31690
1.21600     0.65713     1.04600     0.32130
1.21600     0.65713     1.04200     0.32030
1.21600     0.65713     1.03900     0.31640
1.21600     0.65713     1.05100     0.32110
1.21600     0.65713     1.03100     0.31720
1.21700     0.65767     1.02400     0.31760
1.21700     0.65767     1.03900     0.31790
1.21700     0.65767     1.03400     0.31670
1.21700     0.65767     1.05600     0.32010
1.21800     0.65821     1.04100     0.31690
1.21800     0.65821     1.04300     0.31730
1.21900     0.65875     1.05900     0.32000
1.21900     0.65875     1.04700     0.31960
1.21900     0.65875     1.04800     0.32130
1.21900     0.65875     1.05800     0.32030
1.21900     0.65875     1.00900     0.31440
1.21900     0.65875     1.03100     0.31620
1.22000     0.65929     1.02500     0.31830
1.22100     0.65983     1.04700     0.32080
1.22200     0.66037     1.05700     0.31990
1.22200     0.66037     1.00500     0.31380
1.22300     0.66091     1.00400     0.31320
1.22500     0.66199     1.00700     0.31350
1.22600     0.66253     1.00100     0.31380
1.22600     0.66253     1.00300     0.31390
1.22600     0.66253     1.00000     0.31340
1.22700     0.66307     0.99930     0.31300
```

Figure 13. Example Data File with File Header

This file contains the filenames for all the data files that are included in the High Reynolds Number Pump (HIREP) Data Bank. These files are cross-referenced to the corresponding figure numbers for both the ASME Journal of Fluids Engineering article:

"An Experimental Investigation of the Flow through an Axial Flow Pump" by W. C. Zierke, W. A. Straka and P. D. Taylor

and the much more detailed Penn State University / Applied Research Laboratory Report:

"The High Reynolds Number Flow Through An Axial-Flow" by W. C. Zierke, W. A. Straka and P. D. Taylor, PSU/ARL Technical Report No. TR 93-12, November 1993

DATA BANK DATA FILES:

TR 93-12 Figure #	J.F.E. Article Figure #	DATA FILE NAMES
14		INLET.DAT, INLETSCM.DAT
15	3	INLET.DAT, INLETSCM.DAT
17	4	IGVPS10.DAT, IGVPS30.DAT, IGVPS50.DAT, IGVPS70.DAT, IGVPS90.DAT
18		IGVPS10.DAT, IGVPS30.DAT, IGVPS50.DAT, IGVPS70.DAT, IGVPS90.DAT
28a	5a	IGVLST01.DAT, IGV5HP01.DAT
b		IGVLST02.DAT, IGV5HP02.DAT
c		IGVLST03.DAT, IGV5HP03.DAT
d		IGVLST04.DAT
e		IGVLST05.DAT, IGV5HP05.DAT
f		IGVLST06.DAT, IGV5HP06.DAT
g		IGVLST07.DAT, IGV5HP07.DAT
h		IGVLST08.DAT, IGV5HP08.DAT
i	5b	IGVLST09.DAT, IGV5HP09.DAT
j		IGVLST10.DAT, IGV5HP10.DAT
k		IGVLST11.DAT, IGV5HP11.DAT
l		IGVLST12.DAT, IGV5HP12.DAT
29a		IGVWK-01.DAT, IGVWK-02.DAT, IGVWK-03.DAT, IGVWK-05.DAT
b		IGVWK-06.DAT, IGVWK-07.DAT, IGVWK-08.DAT, IGVWK-09.DAT
30b		WAKEVECT.DAT
31		WAKEVECT.DAT
32		RAD-5HP.DAT, RAKE-5HP.DAT, IGVEXSCM.DAT
33		RAD-5HP.DAT, RAKE-5HP.DAT, IGVEXSCM.DAT
34		IGVEXLDV.DAT, IGVEXSCM.DAT
39		IGVEXLDV.DAT
40		IGVEXLDV.DAT
41		IGVEXLDV.DAT
b		319DH506.DAT, POTLST06.DAT
c		319DH505.DAT, POTLST05.DAT
d		319DH504.DAT, POTLST04.DAT
e		319DH503.DAT, POTLST03.DAT
f		319DH502.DAT, POTLST02.DAT
g		319DH501.DAT
44		ROTPS10.DAT, ROTPS30.DAT, ROTPS50.DAT, ROTPS70.DAT, ROTPS90.DAT
45		ROTPS10.DAT, ROTPS30.DAT, ROTPS50.DAT, ROTPS70.DAT, ROTPS90.DAT
46	7	POWER.DAT
47		POWER.DAT
56a		331DH1**.DAT (where ** = 05 to 20)
b		401DH1**.DAT (where ** = 01 to 31)
c	8	330DH1**.DAT (where ** = 01 to 30)
57a		331DH1**.DAT (where ** = 05 to 20)
b		401DH1**.DAT (where ** = 01 to 31)
c		330DH1**.DAT (where ** = 01 to 30)
58a		DH201ST.DAT, DH202ST.DAT, DH203ST.DAT, DH204ST.DAT
b		DH205ST.DAT, DH206ST.DAT, DH207ST.DAT
59		330DH103.DAT, 330DH106.DAT, 330DH108.DAT 330DH109.DAT, 330DH111.DAT, 330DH113.DAT
60		330DH103.DAT, 330DH106.DAT, 330DH108.DAT 330DH109.DAT, 330DH111.DAT, 330DH113.DAT
61		330DH103.DAT, 330DH106.DAT, 330DH108.DAT 330DH109.DAT, 330DH111.DAT, 330DH113.DAT
62		330DH103.DAT, 330DH106.DAT, 330DH108.DAT 330DH109.DAT, 330DH111.DAT, 330DH113.DAT
63a		DH331LDV.DAT, ROTEXSCM.DAT
b		DH401LDV.DAT, ROTEXSCM.DAT
c		DH330LDV.DAT, ROTEXSCM.DAT
64	9	KIEL-14.DAT, KIEL-22.DAT
66		UNSTEAD2.DAT
67		UNSTEAD1.DAT
72a		DH401LDV.DAT
b		DH330LDV.DAT
73a		DH401LDV.DAT
b		DH330LDV.DAT
74a		331DH1**.DAT (where ** = 05 to 20)
b		401DH1**.DAT (where ** = 01 to 31)
c		330DH1**.DAT (where ** = 01 to 30)
75a		331DH1**.DAT (where ** = 05 to 20)
b		401DH1**.DAT (where ** = 01 to 31)
c		330DH1**.DAT (where ** = 01 to 30)
76a		DH401LDV.DAT
b		DH330LDV.DAT
84		VORT1-TN.DAT, VORT2-TN.DAT, VORT3-TN.DAT
85		VORT1-AX.DAT, VORT2-AX.DAT, VORT3-AX.DAT

Figure 14. Cross-Reference of Filenames with Figure Numbers

The Pennsylvania State University
Applied Research Laboratory
P.O. Box 30
State College, PA 16804